

Thresholds for hanger slackening and cable shortening in the Melan equation for suspension bridges

Filippo Gazzola - Gianmarco Sperone
Dipartimento di Matematica, Politecnico di Milano, Italy

Abstract

The Melan equation for suspension bridges is derived by assuming small displacements of the deck and inextensible hangers. We determine the thresholds for the validity of the Melan equation when the hangers slacken, thereby violating the inextensibility assumption. To this end, we preliminarily study the possible shortening of the cables: it turns out that there is a striking difference between even and odd vibrating modes since the former never shorten. These problems are studied both on beams and plates.

1 Introduction

In 1888, the Austrian engineer Josef Melan [6] introduced the so-called deflection theory and applied it to derive the differential equation governing a suspension bridge, modeled as a combination of a string (the sustaining cable) and a beam (the deck), see Figure 1. The beam and the string are connected through hangers. Since the spacing between hangers is usually small relative to the span, the set of the hangers is considered as a continuous membrane connecting the cable and the deck.

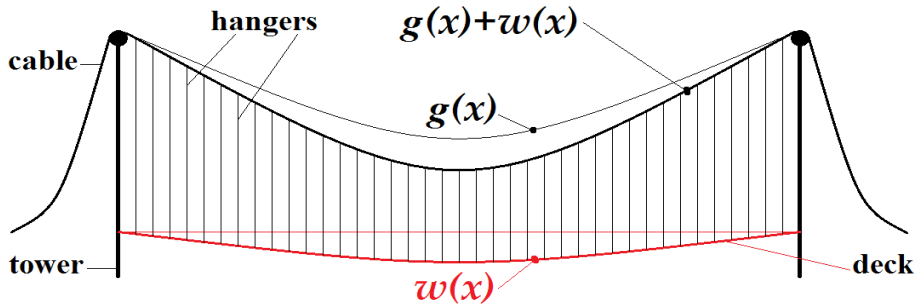


Figure 1: Beam (red) sustained by a cable (black) through parallel hangers.

Let us quickly outline how the Melan equation is derived; we follow here [15, VII.1]. We denote by L the length of the beam at rest (the distance between towers) and $x \in (0, L)$ the position on the beam; $p = p(x)$ the live load and $-q < 0$ the dead load per unit length applied to the beam; $g = g(x)$ the displacement of the cable due to the dead load $-q$; L_c the length of the cable subject to the dead load $-q$; A the cross-sectional area of the cable and E_c its modulus of elasticity; H the horizontal tension in the cable, when subject to the dead load $-q$ only; EI the flexural rigidity of the beam; $w = w(x)$ the displacement of the beam due to the live load p ; $h = h(w)$ the additional tension in the cable produced by the live load p .

When the system is only subject to the action of dead loads, the cable is in position $g(x)$ while the unloaded beam is in the horizontal position $w \equiv 0$, see Figure 1. The cable is adjusted in such a way that it carries its own weight, the weight of the hangers and the weight of the deck (beam) without producing a bending moment in the beam, so that all additional deformations of the cable and the beam due to live loads are small. The cable is considered as a perfectly flexible string subject to vertical dead and live loads. The string is subject to a downwards vertical constant dead load $-q$ and the horizontal component $H > 0$ of the tension remains constant. If the mass of the cable is neglected, then the dead load is distributed per horizontal unit. The resulting equation simply reads $Hg''(x) = q$ (see [15, (1.3),VII]) so that the cable takes the shape of a parabola with a \cup -shaped graph. If the endpoints of the string (top of the towers) are at the same level $\gamma > 0$ (as in suspension bridges, see again Figure 1), then the solution g and the length L_c of the cable are given by:

$$g(x) = \gamma + \frac{q}{2H}x(x-L), \quad g'(x) = \frac{q}{H}\left(x - \frac{L}{2}\right), \quad g''(x) = \frac{q}{H}, \quad \forall x \in (0, L), \quad (1)$$

$$L_c = \int_0^L \sqrt{1 + g'(x)^2} dx. \quad (2)$$

The elastic deformation of the hangers is usually neglected, so that the function w describes both the displacements of the beam and of the cable from its equilibrium position g . This classical assumption is justified by precise studies on linearized models, see e.g. [5]. When the live load p is added, a certain amount p_1 of p is carried by the cable whereas the remaining part $p - p_1$ is carried by the bending stiffness of the beam. In this case, it is well-known [6, 15] that the equation for the displacement w of the beam is

$$EI w''''(x) = p(x) - p_1(x) \quad \forall x \in (0, L). \quad (3)$$

At the same time, the horizontal tension of the cable is increased to $H + h(w)$ and the deflection w is added to the displacement g . Hence, according to (1), the equation which takes into account these conditions reads

$$(H + h(w))(g''(x) + w''(x)) = q - p_1(x) \quad \forall x \in (0, L). \quad (4)$$

Then, by combining (1)-(3)-(4), we obtain

$$EI w''''(x) - (H + h(w)) w''(x) - \frac{q}{H} h(w) = p(x) \quad \forall x \in (0, L), \quad (5)$$

which is known in literature as the **Melan equation** [6, p.77]. The beam representing the bridge is hinged at its endpoints, which means that the boundary conditions to be associated to (5) are

$$w(0) = w(L) = w''(0) = w''(L) = 0. \quad (6)$$

Theoretical results on the Melan equation (5) are quite demanding [3, 4] and this is the reason why it has attracted the attention of numerical analysts [9, 10, 11, 16]. In this paper we analyze and quantify the two main nonlinear (and challenging) behaviors of (5). The first one is the additional tension of the cable, $h(w)$ which is a nonlocal term and is proportional to the length increment of the cable. Depending on the deflection of the beam, the cable may vary its shape and tension, and such phenomenon is studied in Section 2 where we compute the exact thresholds of shortening, depending on the deflection w . In Theorem 2.1 we show that there is a striking difference between the even and odd vibrating modes of the beam. The second source of nonlinearity is the possible slackening of the hangers which, however, is not considered in (5) due to the assumption of inextensibility of the hangers. Indeed, w in (5) aims to represent both the deflections of the beam and of the cable, implying that the cable reaches the new position $g + w$. But since the hangers do not resist to compression, they may slacken so that the cable and the beam move independently and w will no longer represent the displacement of the cable from

its original position. This phenomenon is analyzed in detail in Section 3 where we suggest an improved version of (5) which also takes into account the slackening of the hangers, see (15). In Section 4 we extend this study to a partially hinged rectangular plate aiming to model the deck of a bridge and thereby having two opposite edges completely free: we view these free edges as beams sustained by cables and governed by the Melan equation. The results are complemented with some enlightening figures.

2 Thresholds for cable shortening in a beam model

A given displacement of the deck $w \in C^1([0, L], \mathbb{R})$ generates an additional tension $h(w)$ in the cable that is proportional to the increment of length of the cable $\Gamma(w)$, that is,

$$h(w) = \frac{E_c A}{L_c} \Gamma(w) \quad \text{where} \quad \Gamma(w) = \int_0^L \left[\sqrt{1 + (w'(x) + g'(x))^2} - \sqrt{1 + g'(x)^2} \right] dx. \quad (7)$$

Definition 2.1. *We say that a displacement w **shortens** the cable if $\Gamma(w) < 0$.*

There are at least three rude ways to approximate $h(w)$, by replacing $\Gamma(w)$ with

$$-\frac{q}{H} \int_0^L w(x) dx, \quad -\frac{q}{H} \int_0^L w(x) dx + \int_0^L \frac{w'(x)^2}{2} dx, \quad -\frac{q}{H} \int_0^L \frac{w(x)}{\left[1 + \frac{g^2}{H^2} \left(x - \frac{L}{2}\right)^2\right]^{3/2}} dx.$$

These approximations are obtained through an erroneous argument. While introducing (5), Biot-von Kármán [15] warn the reader by writing *whereas the deflection of the beam may be considered small, the deflection of the string, i.e., the deviation of its shape from a straight line, has to be considered as of finite magnitude*. However, they later decide to *neglect $g'(x)^2$ in comparison with unity*. A similar mistake with a different result is repeated by Timoshenko [13, 14]. These approximations may lead to an average error of about 5% for $h(w)$. Around 1950 the civil and structural German engineer Franz Dischinger emphasized the dramatic consequences of bad approximations on the structures and 5% turns out to be a too large error. Moreover, since related numerical procedures are very unstable, see [3, 9, 10, 11], also from a mathematical point of view one should analyze the term $h(w)$ with extreme care.

Since the displacement of the deck w , created by a live load p , is the solution of the Melan equation (5), we study here which loads yield a shortening of the cable. In particular, we analyze the fundamental modes of vibration of the beam so that we consider the following class of live loads:

$$p_n(x) = \rho \left(\frac{n\pi}{L}\right)^2 \left\{ \left(\frac{n\pi}{L}\right)^2 EI + H + h\left(\rho \sin\left(\frac{n\pi x}{L}\right)\right) \right\} \sin\left(\frac{n\pi x}{L}\right) - \frac{q}{H} h\left(\rho \sin\left(\frac{n\pi x}{L}\right)\right) \quad \forall n \in \mathbb{N}, \quad (8)$$

for varying values of $\rho \in \mathbb{R}$. The load p_n consists of a negative constant part $-\frac{q}{H} h(\rho \sin(\frac{n\pi x}{L}))$ and a part that is proportional to the fundamental vibrating modes of the beam $\sin(\frac{n\pi x}{L})$, which are the eigenfunctions of the following eigenvalue problem:

$$v''''(x) = \lambda v(x) \quad (0 < x < L), \quad v(0) = v(L) = v''(0) = v''(L) = 0. \quad (9)$$

The reason of this choice for p_n is that, after some computations, one sees that the resulting displacement w_n (solution of (5)) is proportional to a vibrating mode:

$$w_n(x) = \rho \sin\left(\frac{n\pi x}{L}\right) \quad \forall x \in [0, L]. \quad (10)$$

Whence, $|\rho|$ measures the amplitude of oscillation of the vibrating mode w_n . For every $n \in \mathbb{N}$, we put $\Gamma_n(\rho) := \Gamma(w_n)$ and from (7) we infer that

$$\Gamma_n(\rho) = \int_0^L \sqrt{1 + \left[\frac{q}{H} \left(x - \frac{L}{2} \right) + \frac{n\pi}{L} \rho \cos \left(\frac{n\pi x}{L} \right) \right]^2} dx - L_c \quad \forall \rho \in \mathbb{R}. \quad (11)$$

In the next result we emphasize a striking difference between even and odd modes.

Theorem 2.1. *Assume that $\frac{q}{H} < \frac{2}{5}$.*

- *If $n \geq 1$ is even, then $\Gamma_n(\rho) \geq 0$ for all ρ ; therefore, an even vibrating mode cannot shorten the cable.*
- *If $n \geq 1$ is odd, then there exists a (unique) critical value $\rho_n^* > 0$ such that $\Gamma_n(\rho_n^*) = 0$ and $\Gamma_n(\rho) < 0$ for all $\rho \in (0, \rho_n^*)$; therefore, odd vibrating modes shorten the cable when their amplitude of oscillation ρ is within this interval.*

Theorem 2.1 is proved in Section 5. The assumption $q/H < 2/5$ in Theorem 2.1 is verified in the vast majority of real suspension bridges. For instance, for the numerical data employed in [16], it happens that $q/H = 1.739 \times 10^{-3} [m^{-1}]$. Moreover, as reported in [8, Section 15.17], the sag-span ratio in a suspension bridge always lies in the range $(\frac{1}{12}, \frac{1}{8})$. In view of (1), this means that

$$\frac{L}{12} < g(0) - g\left(\frac{L}{2}\right) < \frac{L}{8} \quad \text{or, equivalently,} \quad \frac{2}{3L} < \frac{q}{H} < \frac{1}{L}.$$

Therefore, the assumption $\frac{q}{H} < \frac{2}{5}$ is valid for any suspension bridges with a span of at least 2.5 [m]! In any case, numerical results seem to show that the assumption $\frac{q}{H} < \frac{2}{5}$ is not necessary for the validity of Theorem 2.1.

Related to ρ_n^* , as characterized by Theorem 2.1, we introduce the quantity

$$\xi_n^* = \rho_n^* \left(\frac{n\pi}{L} \right)^2 \left\{ \left(\frac{n\pi}{L} \right)^2 EI + H + \frac{E_c A}{L_c} \Gamma(\rho_n^* \sin(\frac{n\pi x}{L})) \right\} \quad \forall n \in \mathbb{N}, \quad (12)$$

which is the amplitude of oscillation of the live load p_n in (8) that generates the critical oscillation $w_n^*(x) = \rho_n^* \sin(\frac{n\pi x}{L})$. Throughout this paper, as far as numerical data are needed, we use the parameters taken from [16]:

$$L = 460 [m], \quad EI = 57 \times 10^6 [kN \cdot m], \quad E_c A = 36 \times 10^6 [kN], \quad \frac{q}{H} = 1.739 \times 10^{-3} [m^{-1}]. \quad (13)$$

Table 1 shows the critical values of ρ_n^* and ξ_n^* (according to Theorem 2.1 and (12)), as functions of some odd values of $n \in \mathbb{N}$.

n	1	3	5	7	9	11	13	15	17	19
ρ_n^*	94.807	3.056	0.657	0.239	0.112	0.061	0.037	0.024	0.016	0.011
ξ_n^*	444.016	156.115	125.811	124.578	132.962	145.676	160.734	177.192	194.559	212.620

Table 1: Critical coefficients for cable shortening in odd-vibrating modes.

As stated in Theorem 2.1, even modes never shorten the cable. This *does not* mean that odd modes are “worse” or more prone to elongate the cable. On the contrary, thinking of a periodic-in-time oscillation proportional to a vibrating mode (10), that is,

$$\rho(t) \sin\left(\frac{n\pi x}{L}\right) \quad \forall x \in [0, L], \quad \forall t > 0,$$

with $\rho(t)$ varying between $\pm\bar{\rho}$, we reach the opposite conclusion. To see this, in Figure 2 we plot the graphs of Γ_2 and Γ_3 and we see that

$$\max\{\Gamma_3(\bar{\rho}), \Gamma_3(-\bar{\rho})\} > \max\{\Gamma_2(\bar{\rho}), \Gamma_2(-\bar{\rho})\} = \Gamma_2(\bar{\rho}).$$

Therefore, even if the cable shortens when $\rho(t) \in (0, \rho_3^*)$ for the third mode, the cable itself elongates more than for the second mode when $\rho(t) < 0$. We come back to this issue in Section 4.

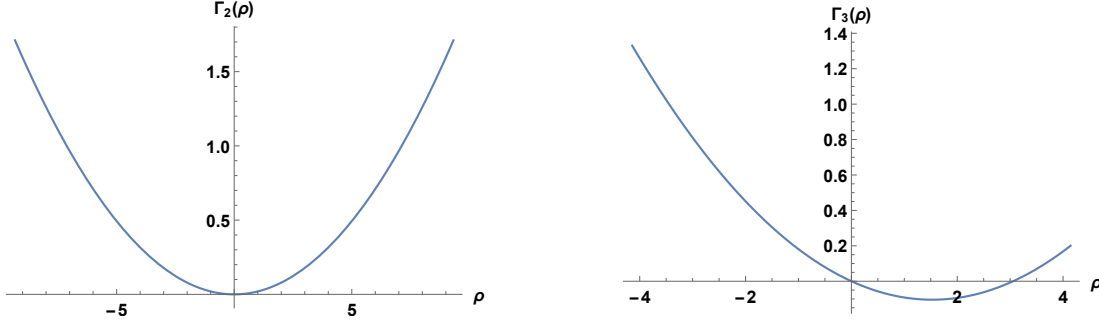


Figure 2: Increment of cable length in the second (left) and third (right) vibrating modes.

3 Thresholds for hangers slackening in a beam model

In this section we estimate the thresholds that provoke the slackening of some hangers. Since the hangers resist to extension but not to compression, if the deck goes too high above its equilibrium position, then *the hangers may no longer be considered as rigid inextensible bars*. In particular, they will not push upwards the cable in such a way that it loses convexity: the general principles governing the deformation of a finite-length cable under the action of a downwards vertical load (see [15, (1.3), VII]) indicate that the cable remains convex. This means that if $g + w$ is not convex, then it *does not* describe the position of the cable anymore.

In order to explain how the Melan equation (5) should be modified in case of hanger slackening we briefly recall the concept of *convexification* which can be formalized in several equivalent ways, see [1, (3.2), I] for full details.

Let $I \subset \mathbb{R}$ be a compact interval. The convexification f^{**} of a continuous function $f : I \rightarrow \mathbb{R}$ is:

- the pointwise supremum of all the affine functions everywhere less than f ;
- the pointwise supremum of all the convex functions everywhere less than f ;
- the largest convex function everywhere less than or equal to f ;
- the convex function whose epigraph is the closed convex hull of the epigraph of f ;
- the second Fenchel conjugate of f , that is,

$$f^{**}(x) = \sup_{y \in \mathbb{R}} \{xy - f^*(y)\} \quad \forall x \in I, \quad \text{where} \quad f^*(y) = \max_{x \in I} \{yx - f(x)\} \quad \forall y \in \mathbb{R}.$$

This notion enables us to give the following:

Definition 3.1. *We say that a displacement w **slackens** the hangers in some (nonempty) interval $(a, b) \subset [0, L]$ if the graph of*

$$z := g + w \tag{14}$$

*lies strictly above that of its convexification z^{**} in (a, b) . Then, the **slackening region** $\mathcal{S} \subset [0, L]$ is the union of all the slackening intervals, that is,*

$$\mathcal{S} = \{x \in (0, L) \mid z(x) > z^{**}(x)\}.$$

In the slackening region, not only the Melan equation (5) is incorrect but also (3) fails since *the whole amount of live load is carried by the beam*: one has $p_1(x) = 0$ for all $x \in \mathcal{S}$. Therefore (5) should be replaced with the more reliable equation

$$EI w''''(x) + \left(\chi_{\mathcal{S}}(w) - 1\right) \left((H + h(w)) w''(x) + \frac{q}{H} h(w) \right) = p(x) \quad \forall x \in (0, L) \tag{15}$$

where $\chi_{\mathcal{S}}(w)$ is the characteristic function (that depends on w) of the slackening region \mathcal{S} , see Definition 3.1. We summarize these results in the following statement.

Proposition 3.1. *In absence of slackening ($\mathcal{S} = \emptyset$) the two equations (5) and (15) coincide; in this case, the solution w represents the displacement of the beam whereas z in (14) represents the position of the cable.*

*In presence of slackening ($\mathcal{S} \neq \emptyset$) the correct equation is (15) and the position of the cable is described by z^{**} .*

The term $(\chi_{\mathcal{S}}(w) - 1)$ adds a further nonlinearity to the Melan equation (5). As far as we are aware, there is no general theory to tackle equations such as (15). It would therefore be interesting to study its features in detail.

Although the exact slackening region is difficult to determine, it is clear that the non-convexity intervals of z in (14) represent proper subsets of these regions. Therefore, we have

Proposition 3.2. *Let w be the solution of (15) and let z be as in (14). If $\mathcal{S} \neq \emptyset$, then*

$$\{x \in (0, L); z''(x) \leq 0\} \subsetneq \mathcal{S}.$$

We now apply Proposition 3.1 to the case of the loads p_n in (8).

Proposition 3.3. *Let p_n and w_n be as in (8) and (10). Let*

$$C_n^* := \frac{q}{H} \left(\frac{L}{n\pi} \right)^2 \quad \forall n \in \mathbb{N}. \quad (16)$$

Slackening occurs if and only if

$$\rho > C_1^* \text{ when } n = 1, \quad |\rho| > C_n^* \text{ when } n \geq 2; \quad (17)$$

*in this case, the position of the cable is described by z_n^{**} (with $z_n = g + w_n$).*

The proof of Proposition 3.3 is fairly simple. The slackening region of w_n is nonempty if and only if there exists $x \in (0, L)$ such that $z_n''(x) < 0$, where

$$z_n(x) = g(x) + w_n(x) = \gamma + \frac{q}{2H}x(x - L) + \rho \sin\left(\frac{n\pi x}{L}\right) \quad \forall x \in [0, L].$$

This property translates into

$$\exists x \in (0, L) \quad \text{such that} \quad \rho \sin\left(\frac{n\pi x}{L}\right) > C_n^*,$$

which is equivalent to (17).

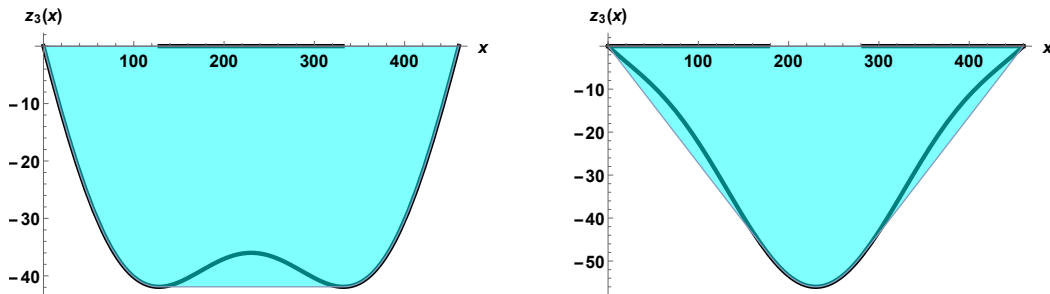


Figure 3: Slackening of the third vibrating mode when $\rho_3 < -C_3^*$ (left) and when $\rho_3 > C_3^*$ (right).

Since it is by far nontrivial to determine explicitly the convexification of z_n and the slackening region \mathcal{S}_n , we follow a numerical-geometrical approach, that is, we plot the closed convex hull of the epigraph of z_n . We take again the numerical values (13). In order to illustrate the procedure, consider the function z_3 (with $\gamma = 0$, since we are only interested in the shape of the curve), whose slackening threshold is $C_3^* \approx 4.1426$. By putting amplitudes of $\rho_3 = \pm 10$, we obtained the graphs of z_3 in Figure 3 where the slackening intervals have been highlighted over the horizontal axis, and the closed convex hull of the epigraph of z_3 has been shaded. Similarly, by putting amplitudes of $\rho_5 = \pm 5$, we obtained the plots displayed in Figure 4 for the graphs of z_5 (for which $C_5^* \approx 1.4913$):

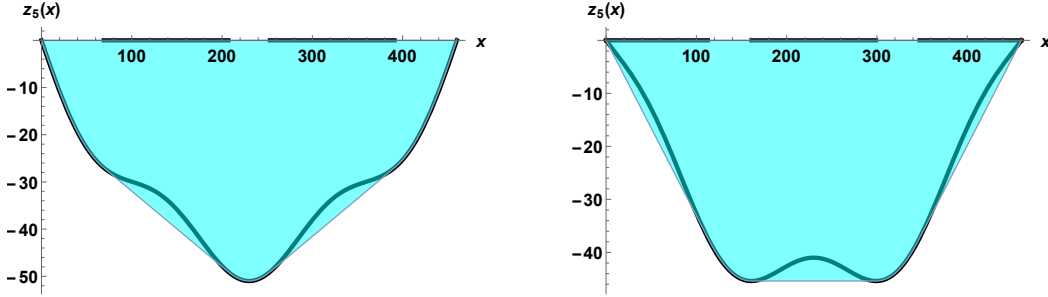


Figure 4: Slackening of the fifth vibrating mode when $\rho_5 < -C_5^*$ (left) and when $\rho_5 > C_5^*$ (right).

It is worthwhile noticing that the hangers slackening in even modes occurs asymmetrically with respect to the center of the beam but, at the same time, symmetrically with respect to the value of ρ_n . To clarify this point, in Figure 5 we display the graphs of z_2 (where $C_2^* \approx 9.3208$) when $\rho_2 = -20$, and of z_4 (where $C_4^* \approx 2.3301$) when $\rho_4 = 8$. The remaining figures when $\rho_2 > C_2^*$ or $\rho_4 < -C_4^*$ may be obtained by simply reflecting the curves with respect to the center of the beam.

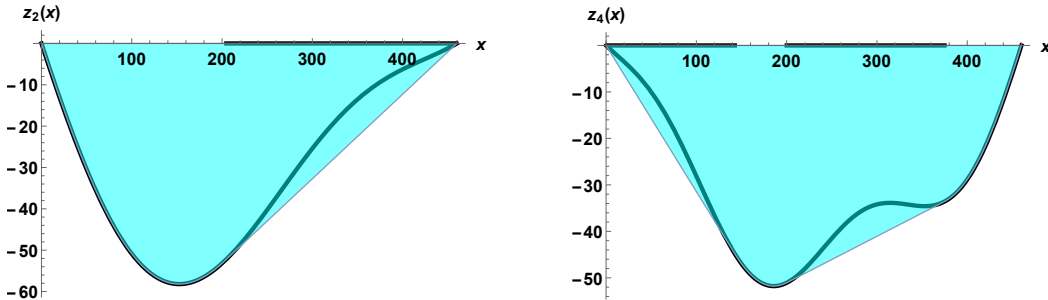


Figure 5: Slackening of the second vibrating mode when $\rho_2 < -C_2^*$ (left), and of the fourth vibrating mode when $\rho_4 > C_4^*$ (right).

The numerical values of C_n^* for $n \leq 10$ are reported in Table 2 where we used the parameters as in (13).

One last issue must be addressed. In some of the pictures in Figures 3, 4 and 5 we observe that the endpoints of the deck $x = 0$ and $x = L$ actually belong to the slackening region \mathcal{S}_n . This is clearly a physically impossible situation since the hangers are not expected to slacken at the endpoints of the beam. Geometrically, one expects instead that the tangent lines to the curve at the endpoints of the beam lie strictly below the graph of z_n in $(0, L)$, that is:

$$z_n(x) > \max\{z_n'(0)x, z_n'(L)(x - L)\} \quad \forall x \in (0, L), \quad \forall n \in \mathbb{N}. \quad (18)$$

Clearly, condition (18) is not satisfied for large values of $|\rho_n|$, but it remains valid even when $|\rho_n|$ is slightly larger than the slackening (and convexity) threshold (16). For the first ten vibrating modes, we

numerically computed the threshold ρ_n^{**} that ensures condition (18), when $|\rho_n| \leq \rho_n^{**}$ (if n is even) and $\rho_n \leq \rho_n^{**}$ (if n is odd), with the parameters as in (13). We obtained the second line in Table 2.

n	1	2	3	4	5	6	7	8	9	10
C_n^*	37.283	9.321	4.143	2.330	1.491	1.035	0.761	0.582	0.460	0.372
ρ_n^{**}	58.564	14.641	6.507	3.660	2.342	1.626	1.195	0.915	0.723	0.585

Table 2: Thresholds for non-convexity and hangers slackening in the first ten vibrating modes.

4 Behavior of cables and hangers in a plate model

The deck of a real bridge cannot be described by a simple (one-dimensional) beam since it fails to display torsional oscillations. In this section we take advantage of the results so far obtained in order to analyze the vibrating modes of a rectangular plate $\Omega = (0, \pi) \times (-\ell, \ell)$ ($2\ell > 0$ is the width of the plate and $2\ell \ll \pi$); for simplicity, we take here $L = \pi$. Specifically, we consider a partially hinged plate whose elastic energy is given by the Kirchhoff-Love functional, see [7, 12] for discussions on the boundary conditions and updated derivation of the corresponding Euler-Lagrange equation. From [2] we know that the vibrating modes of the plate Ω are obtained by solving the following eigenvalue problem

$$\begin{cases} \Delta^2 u = \lambda u & \text{for } (x, y) \in \Omega \\ u = u_{xx} = 0 & \text{for } (x, y) \in \{0, \pi\} \times (-\ell, \ell) \\ u_{yy} + \sigma u_{xx} = u_{yyy} + (2 - \sigma)u_{xxy} = 0 & \text{for } (x, y) \in (0, \pi) \times \{-\ell, \ell\}, \end{cases} \quad (19)$$

where $\sigma \in (0, \frac{1}{2})$ is the Poisson ratio. The boundary conditions for $x = 0$ and $x = \pi$ show that the short edges of the plate are hinged, while the conditions for $y = \pm\ell$ show that the plate is free on the long edges. Problem (19) is the two-dimensional counterpart of (9). From [2] we also know that the eigenvalues of (19) may be ordered in an increasing sequence of strictly positive numbers diverging to $+\infty$. Correspondingly, the eigenfunctions are identified by two indices $m, k \in \mathbb{N}_+$ and they have one of the following forms:

$$\begin{aligned} W_{m,k}(x, y) &= \varphi_{m,k}(y) \sin(mx) & \text{with corresponding eigenvalue } \nu_{m,k}, \\ \bar{W}_{m,k}(x, y) &= \psi_{m,k}(y) \sin(mx) & \text{with corresponding eigenvalue } \mu_{m,k}. \end{aligned}$$

The $\varphi_{m,k}$ are odd while the $\psi_{m,k}$ are even and this is why the $W_{m,k}$ are called *torsional* eigenfunctions while the $\bar{W}_{m,k}$ are called *longitudinal* eigenfunctions. The main difference between these two classes is precisely that $\bar{W}_{m,k}(x, \ell) = \bar{W}_{m,k}(x, -\ell)$ so that the free edges $y = \pm\ell$ are in the same position for longitudinal vibrations, while $W_{m,k}(x, \ell) = -W_{m,k}(x, -\ell)$ so that the free edges are in opposite positions for torsional vibrations.

We first deal with the slightly more complicated case of torsional vibrating modes. Then the eigenvalues $\nu_{m,k}$ are the (ordered) solutions $\lambda > m^4$ of the following equation:

$$\sqrt{\lambda^{1/2} - m^2} [\lambda^{1/2} + (1 - \sigma)m^2]^2 \tanh(\ell \sqrt{\lambda^{1/2} + m^2}) = \sqrt{\lambda^{1/2} + m^2} [\lambda^{1/2} - (1 - \sigma)m^2]^2 \tanh(\ell \sqrt{\lambda^{1/2} - m^2}),$$

while the function $\varphi_{m,k}$ may be taken as

$$\varphi_{m,k}(y) = [\nu_{m,k}^{1/2} - (1 - \sigma)m^2] \frac{\sinh\left(y \sqrt{\nu_{m,k}^{1/2} + m^2}\right)}{\sinh\left(\ell \sqrt{\nu_{m,k}^{1/2} + m^2}\right)} + [\nu_{m,k}^{1/2} + (1 - \sigma)m^2] \frac{\sin\left(y \sqrt{\nu_{m,k}^{1/2} - m^2}\right)}{\sin\left(\ell \sqrt{\nu_{m,k}^{1/2} - m^2}\right)},$$

see [2]. In particular, $\varphi_{m,k}(\ell) = 2\sqrt{\nu_{m,k}} = -\varphi_{m,k}(-\ell)$.

We view both the free edges of the plate $y = \pm\ell$ as beams connected to a cable and governed by the modified Melan equation (15). Then we take the following function as a solution of (15):

$$w_{m,k}(x) := \alpha W_{m,k}(x, \ell) = \alpha \varphi_{m,k}(\ell) \sin(mx) = 2\alpha \sqrt{\nu_{m,k}} \sin(mx) \quad \forall x \in [0, \pi], \quad (20)$$

for $m, k \in \mathbb{N}$ and $\alpha \in \mathbb{R}$, a function that belongs to the family of eigenfunctions of (9), see (10), assuming that $L = \pi$. As already mentioned, together with $w_{m,k}$ in (20), for torsional modes one needs to consider also its companion $-w_{m,k}$.

For longitudinal modes, one has to replace $w_{m,k}$ in (20) with

$$\bar{w}_{m,k}(x) := \alpha \bar{W}_{m,k}(x, \ell) = \alpha \psi_{m,k}(\ell) \sin(mx) \quad \forall x \in [0, \pi], \quad (21)$$

where $\psi_{m,k}(\ell)$ depends on the longitudinal eigenvalue $\mu_{m,k}$ of (19); see [2] for the precise characterization of $\mu_{m,k}$. For longitudinal modes, the behavior is the same on the two opposite edges.

The above discussion, combined with Theorem 2.1, yields the following statement.

Proposition 4.1. *Assume that $\frac{q}{H} < \frac{2}{5}$.*

- *If $m \geq 1$ is even, then the vibrating mode (either torsional or longitudinal) cannot shorten the cable.*
- *If $m \geq 1$ is odd and the mode is longitudinal, then there exists a (unique) critical value $\alpha^* = \alpha_{m,k}^* > 0$ such that for $\alpha \in (0, \alpha^*)$ both the cables are shortened while for other values of α no cable is shortened.*
- *If $m \geq 1$ is odd and the mode is torsional, then there exists a (unique) critical value $\alpha^* = \alpha_{m,k}^* > 0$ such that for $0 < |\alpha| < \alpha^*$ one and only one cable is shortened, while for other values of α no cable is shortened.*

Following the guideline of Section 2, one may then determine the exact critical values $\alpha_{m,k}^*$ (for odd m). It suffices to consider the critical values ρ_n^* from Theorem 2.1 and to take

$$\alpha_{m,k}^* = \frac{\rho_m^*}{\varphi_{m,k}(\ell)} \quad \text{or} \quad \alpha_{m,k}^* = \frac{\rho_m^*}{\psi_{m,k}(\ell)},$$

depending on whether the vibration is torsional or longitudinal.

Regarding slackening and the loss of convexity, the above discussion, combined with Propositions 3.2 and 3.3, yields the following statement.

Proposition 4.2. *Let w be the solution of (15) and assume that one of the free edges of Ω is in position w . Let z be as in (14). If $\mathcal{S} \neq \emptyset$, then*

$$\{x \in (0, L); z''(x) \leq 0\} \subsetneq \mathcal{S}.$$

In particular, if $w_{m,k}$ in (20) (resp. $\bar{w}_{m,k}$ in (21)) is the position of one of the free edges of Ω , then slackening of the hangers on that edge occurs if and only if

$$\alpha_1 > \frac{q}{H\varphi_{1,k}(\ell)} \text{ when } m = 1, \quad |\alpha_m| > \frac{q}{Hm^2\varphi_{m,k}(\ell)} \text{ when } m \geq 2$$

$$\left(\text{resp. } \alpha_1 > \frac{q}{H\psi_{1,k}(\ell)} \text{ when } m = 1, \quad |\alpha_m| > \frac{q}{Hm^2\psi_{m,k}(\ell)} \text{ when } m \geq 2 \right);$$

*in this case, the position of the cable is described by $z_{m,k}^{**}$ (with $z_{m,k} = g + w_{m,k}$, resp. $z_{m,k} = g + \bar{w}_{m,k}$).*

The final step consists in considering the evolution equation modeling the vibrations of the partially hinged rectangular plate Ω . According to [2], this leads to the following fourth-order wave-type equation:

$$\begin{cases} u_{tt} + \Delta^2 u = 0 & \text{for } (x, y, t) \in \Omega \times \mathbb{R}_+ \\ u = u_{xx} = 0 & \text{for } (x, y, t) \in \{0, \pi\} \times (-\ell, \ell) \times \mathbb{R}_+ \\ u_{yy} + \sigma u_{xx} = u_{yyy} + (2 - \sigma)u_{xyy} = 0 & \text{for } (x, y, t) \in (0, \pi) \times \{-\ell, \ell\} \times \mathbb{R}_+. \end{cases} \quad (22)$$

Proposition 4.3. Assume that $\frac{q}{H} < \frac{2}{5}$.

- If $m \geq 1$ is even, then the vibrating mode (either torsional or longitudinal) does not shorten the cables for any $t > 0$.
- If $m \geq 1$ is odd and the mode is longitudinal, then both the cables are shortened if $t \in I_S$ whereas no cable is shortened if $t \in I_N$.
- If $m \geq 1$ is odd and the mode is torsional, then one and only one cable is shortened when $t \in I^S$ whereas no cable is shortened if $t \in I^N$.

Once more we emphasize the striking difference between odd and even modes. Proposition 4.3 is illustrated in Figure 6 by shading the sub-regions of the rectangle $(B, t) \in [-0.0001, 0.0001] \times [0, 0.05]$ in which $t \in I^S$ for the third torsional mode. It turns out that for $0 < |B| \lesssim 0.000032$, for almost every $t > 0$ one (and only one) cable is shortened, whereas for larger values of $|B|$ the white regions (no shortening) have positive measure.

Also the slackening of the hangers (and the loss of convexity) in all the vibrating modes is now observed in a space-time region which periodically-in-time reproduces itself. In order to discuss together the longitudinal and torsional cases, we use the same notation to denote the function to be convexified:

$$z_{m,k}(x, t) = g(x) + v_{m,k}(x, t) \quad (\text{resp. } z_{m,k}(x, t) = g(x) + \bar{v}_{m,k}(x, t)) \quad \forall (x, t) \in (0, \pi) \times \mathbb{R}_+, \quad (27)$$

where $v_{m,k}$ and $\bar{v}_{m,k}$ are as in (25) and (26). Concerning the non-convexity regions, for a given $B \in \mathbb{R}$ they are characterized by the points $(x, t) \in [0, \pi] \times [0, \infty)$ that satisfy the inequality:

$$\frac{\partial^2 z_{m,k}}{\partial x^2}(x, t) \leq 0$$

or, equivalently, by the points $(x, t) \in [0, \pi] \times [0, \infty)$ in which:

$$Bm^2 \varphi_{m,k}(\ell) \cos(\sqrt{\nu_{m,k}} t) \sin(mx) \geq \frac{q}{H} \quad (\text{resp. } Bm^2 \psi_{m,k}(\ell) \cos(\sqrt{\nu_{m,k}} t) \sin(mx) \geq \frac{q}{H}). \quad (28)$$

Notice that inequality (28) defines a region of \mathbb{R}^2 of positive measure only when $|B| > C_{m,k}^*$, where the convexity threshold is now given by:

$$C_{m,k}^* = \frac{q}{Hm^2 \varphi_{m,k}(\ell)} \text{ for the torsional modes, } C_{m,k}^* = \frac{q}{Hm^2 \psi_{m,k}(\ell)} \text{ for the longitudinal modes,}$$

for every integers $m, k \geq 1$. Precisely, given $B \in \mathbb{R}$ and integers m and k , let us put:

$$\alpha_{m,k}(t) = B \cos(\sqrt{\nu_{m,k}} t) \quad (\text{resp. } \alpha_{m,k}(t) = B \cos(\sqrt{\mu_{m,k}} t)) \quad \forall t \geq 0.$$

Then, as a consequence of Proposition 4.2, we obtain the following statement.

Proposition 4.4. Let u be the solution of (22) and assume that one of the free edges of Ω is in position $v_{m,k}$ as in (25) or $\bar{v}_{m,k}$ as in (26). Let $z_{m,k}$ be as in (27), depending on the vibrating mode considered. If $|B| > C_{m,k}^*$, then $\mathcal{S} \neq \emptyset$. Furthermore, whenever $|\alpha_{m,k}(t)| > C_{m,k}^*$ we have:

$$\left\{ x \in (0, \pi) \mid \frac{\partial^2 z_{m,k}}{\partial x^2}(x, t) \leq 0 \right\} \subsetneq \mathcal{S}.$$

More precisely, if $|B| > C_{m,k}^*$ and if $v_{m,k}$ in (25) (resp. $\bar{v}_{m,k}$ in (26)) is the position of one of the free edges of Ω , then slackening of the hangers on that edge occurs for all $t > 0$ such that:

$$\alpha_{1,k}(t) > \frac{q}{H\varphi_{1,k}(\ell)} \text{ when } m = 1, \quad |\alpha_{m,k}(t)| > \frac{q}{Hm^2 \varphi_{m,k}(\ell)} \text{ when } m \geq 2$$

$$\left(\text{resp. } \alpha_{1,k}(t) > \frac{q}{H\psi_{1,k}(\ell)} \text{ when } m = 1, \quad |\alpha_{m,k}(t)| > \frac{q}{Hm^2 \psi_{m,k}(\ell)} \text{ when } m \geq 2 \right);$$

in this case, the position of the cable is described by $z_{m,k}^{**}$, with $z_{m,k} = g + v_{m,k}$ as in (27).

Proposition 4.4 defines the slackening regions in the (x, t) -plane. Since these are difficult to determine explicitly, we focus our attention on the non-convexity regions. As a first example, we take the second torsional mode, whose convexity threshold is $C_{2,1}^* \approx 1.52 \times 10^{-4}$. In this case, setting $B = \pm 2 \times 10^{-4}$ and considering the rectangle $(x, t) \in [0, \pi] \times [0, 0.035]$, we obtained Figure 7.

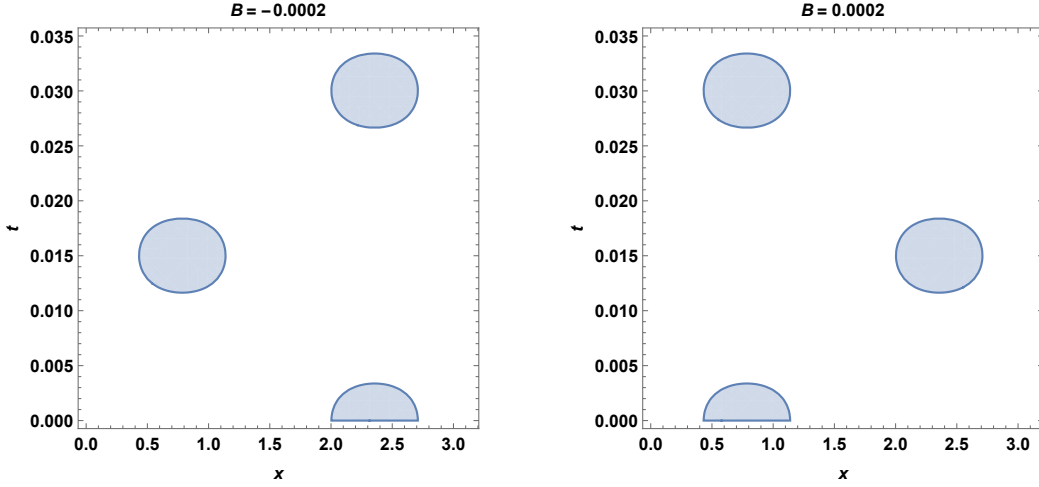


Figure 7: Non-convexity region of the second torsional mode for a time-varying amplitude.

Similar plots are obtained for the function $z_{3,1}$, whose convexity threshold is $C_{3,1}^* \approx 4.5 \times 10^{-5}$. By taking $B = \pm 1 \times 10^{-4}$, we get the following sub-region of the space-time rectangle $(x, t) \in [0, \pi] \times [0, 0.025]$ defined by Proposition 4.4:

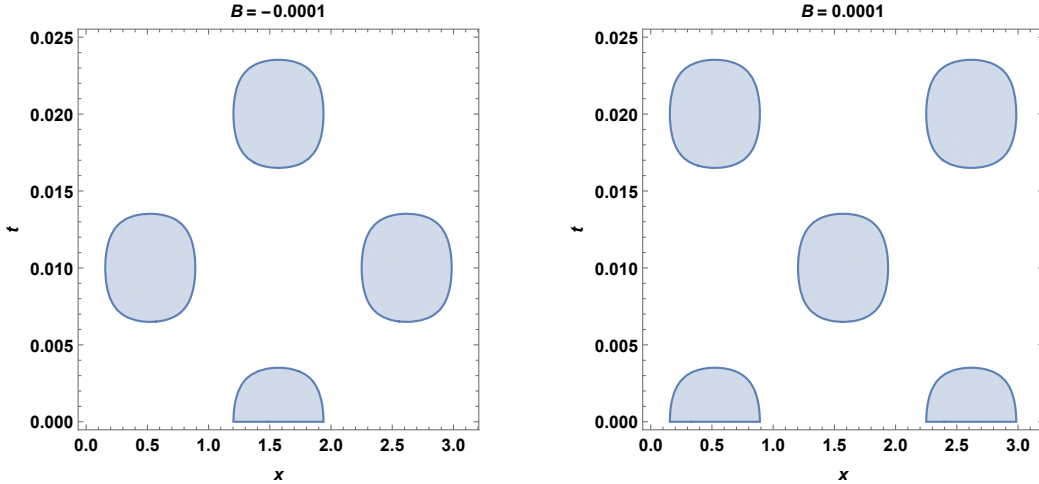


Figure 8: Non-convexity region of the third torsional mode for a time-varying amplitude.

All these plots may also be read by assuming that the right and left pictures represent simultaneously the non-convexity intervals for each cable, as far as torsional vibrations are involved: for any given $t > 0$ one should cross horizontally the two pictures in order to find which part of the interval $(0, \pi)$ of the two cables would be non-convex. In fact, the non-convexity regions are proper subsets of the slackening regions, see Proposition 4.4. Hence, the slackening regions are slightly wider in the x -direction than the “ellipses” in the above plots. This fact is illustrated in Figure 9 where we compare the non-convexity and slackening regions in the third torsional mode:

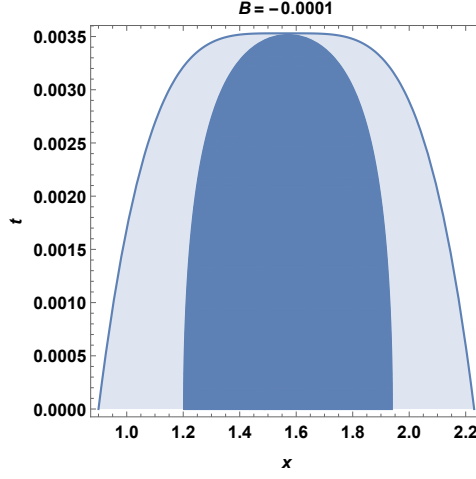


Figure 9: Slackening region for the third torsional mode

5 Proof of Theorem 2.1

The first step is a technical lemma which involves hyper-geometric integrals:

Lemma 5.1. *For odd $n \in \mathbb{N}$ and $0 < \mu < \frac{2}{5}$ we have*

$$G_n := \int_0^{\pi/2} \frac{t \sin(nt)}{\sqrt{1 + (\mu t)^2}} dt \begin{cases} > 0 & \text{if } n \equiv 1 \pmod{4} \\ < 0 & \text{if } n \equiv 3 \pmod{4}. \end{cases} \quad (29)$$

Proof. For $t \in \mathbb{R}$ such that $|t| < \frac{1}{\mu}$, the following power expansion is valid:

$$\frac{1}{\sqrt{1 + (\mu t)^2}} = \sum_{k=0}^{\infty} \binom{-1/2}{k} (\mu t)^{2k}.$$

Therefore, since $\mu < \frac{2}{5}$, for all $t \in \left[0, \frac{\pi}{2}\right]$ we can write:

$$G_n = \sum_{k=0}^{\infty} \binom{-1/2}{k} I_{n,k} \mu^{2k} \quad \forall n \in \mathbb{N}, \quad \text{where} \quad I_{n,k} = \int_0^{\pi/2} t^{2k+1} \sin(nt) dt \quad \forall n, k \in \mathbb{N}. \quad (30)$$

Since we are considering odd values of $n \in \mathbb{N}$, after integrating by parts twice $I_{n,k}$ in (30) we obtain:

$$I_{n,k} = -\frac{2k(2k+1)}{n^2} I_{n,k-1} + \delta(n) \frac{2k+1}{n^2} \left(\frac{\pi}{2}\right)^{2k} \quad \forall k \geq 1,$$

with $I_{n,0} = \frac{\delta(n)}{n^2}$, for every odd $n \in \mathbb{N}$, and:

$$\delta(n) = \begin{cases} 1 & \text{if } n \equiv 1 \pmod{4} \\ -1 & \text{if } n \equiv 3 \pmod{4}. \end{cases} \quad (31)$$

An inductive argument over $k \geq 1$ allows then to deduce

$$I_{n,k} = \delta(n) \sum_{j=0}^k \frac{(-1)^{k+j}}{n^{2(k+1-j)}} \frac{(2k+1)!}{(2j)!} \left(\frac{\pi}{2}\right)^{2j} \quad \forall k \geq 1. \quad (32)$$

Our first claim is that $I_{n,k} > 0$ when $n \equiv 1 \pmod{4}$, and that $I_{n,k} < 0$ when $n \equiv 3 \pmod{4}$, for all $k \in \mathbb{N}$. But, according to (31) and the form of expression (32), it suffices to show that:

$$J_{n,k} := (-1)^k \sum_{j=0}^k \frac{(-1)^j}{(2j)!} \left(\frac{n\pi}{2}\right)^{2j} > 0 \quad \forall n \in \mathbb{N} \text{ odd}, k \geq 1. \quad (33)$$

In order to prove (33), we distinguish two cases.

• **Case (A):** $k > \frac{\sqrt{1+(n\pi)^2} - 7}{4}$. Since $n \in \mathbb{N}$ is odd, we know that

$$0 = \cos\left(\frac{n\pi}{2}\right) = \sum_{j=0}^k \frac{(-1)^j}{(2j)!} \left(\frac{n\pi}{2}\right)^{2j} + \sum_{j=k+1}^{\infty} \frac{(-1)^j}{(2j)!} \left(\frac{n\pi}{2}\right)^{2j}. \quad (34)$$

We put $a_j = \frac{1}{(2j)!} \left(\frac{n\pi}{2}\right)^{2j}$ and observe that, for every $j \geq 1$,

$$\frac{a_j}{a_{j-1}} = \frac{(n\pi)^2}{8j(2j-1)} < 1 \iff j > \frac{\sqrt{1+(n\pi)^2} + 1}{4}.$$

Hence, the Leibniz criterion can be applied to the *tail* series $\sum_{j=k+1}^{\infty} (-1)^j a_j$ if $j > \frac{\sqrt{1+(n\pi)^2} + 1}{4}$. But since the first ratio to be considered is a_{k+2}/a_{k+1} , the Leibniz criterion may be applied whenever

$$k+2 > \frac{\sqrt{1+(n\pi)^2} + 1}{4} \iff k > \frac{\sqrt{1+(n\pi)^2} - 7}{4},$$

which is precisely the case considered. Therefore, the tail series $\sum_{j=k+1}^{\infty} (-1)^j a_j$ has the same sign as $(-1)^{k+1}$. In view of (34), the finite sum $\sum_{j=0}^k (-1)^j a_j$ has the sign of $(-1)^k$, that is, the opposite sign of the tail series. In turn, $J_{n,k} > 0$ in this case, for all odd values of $n \in \mathbb{N}$.

• **Case (B):** $k < \frac{\sqrt{1+(n\pi)^2} - 7}{4}$. We distinguish here further between odd and even values of k . For even $k \in \mathbb{N}$, we may write

$$J_{n,k} = 1 + \sum_{i=1}^{k/2} (a_{2i} - a_{2i-1})$$

and, since $2i \leq k$, all the terms in the sum are positive in view of the assumption of case B. Therefore, $J_{n,k} > 0$ for even k .

For odd $k \in \mathbb{N}$, we may write

$$J_{n,k} = \sum_{i=0}^{\frac{k-1}{2}} (a_{2i+1} - a_{2i})$$

and, since $2i+1 \leq k$, all the terms in the sum are positive in view of the assumption of case B. Therefore, $J_{n,k} > 0$ also for odd k .

Inequality (33) is so proved for all n and k . Let us now fix an integer $n \equiv 1 \pmod{4}$ (the case when $n \equiv 3 \pmod{4}$ follows a completely analogous procedure). As a consequence of (33), we obtain the upper bound:

$$I_{n,k} = -\frac{2k(2k+1)}{n^2} \frac{(2k-1)!}{n^{2k}} J_{n,k-1} + \frac{2k+1}{n^2} \left(\frac{\pi}{2}\right)^{2k} < \frac{2k+1}{n^2} \left(\frac{\pi}{2}\right)^{2k} \quad \forall k \geq 1. \quad (35)$$

Back to (30), we may write:

$$G_n = \frac{1}{n^2} + \sum_{k=1}^{\infty} \binom{-1/2}{k} \left[\sum_{j=0}^k \frac{(-1)^{k+j} (2k+1)!}{n^{2(k+1-j)} (2j)!} \left(\frac{\pi}{2}\right)^{2j} \right] \mu^{2k}. \quad (36)$$

We observe that the binomial coefficient $\binom{-1/2}{k}$ is negative when k is odd and positive otherwise. Furthermore, if we put

$$b_k := \left| \binom{-1/2}{k} \right| \quad \forall k \geq 1,$$

then one has that

$$\frac{b_{k+1}}{b_k} = \frac{2k+1}{2k+2} < 1 \quad \forall k \geq 1, \quad (37)$$

so that $b_k \leq b_1 = 1/2$ for all $k \geq 1$. Since in (36) all the terms in the sum over $j \in \{0, \dots, k\}$ are strictly positive as a consequence of (33), by exploiting (35) and (37) we obtain

$$G_n > \frac{1}{n^2} - \sum_{\substack{k=1 \\ k \text{ odd}}}^{\infty} \frac{1}{2} \frac{2k+1}{n^2} \left(\frac{\mu\pi}{2}\right)^{2k} = \frac{1}{n^2} \left[1 - \frac{1}{2} \sum_{p=0}^{\infty} (4p+3) \left(\frac{\mu\pi}{2}\right)^{4p+2} \right].$$

For every $x \in (-1, 1)$, the geometric series can be differentiated term by term, that is,

$$\frac{d}{dx} \left(\sum_{p=0}^{\infty} x^{4p+3} \right) = \sum_{p=0}^{\infty} (4p+3) x^{4p+2} = \frac{d}{dx} \left(\frac{x^3}{1-x^4} \right) = \frac{x^6 + 3x^2}{(1-x^4)^2} \quad \forall x \in (-1, 1).$$

Hence, we finally infer that

$$G_n > \frac{1}{n^2} \left[1 - \frac{\left(\frac{\mu\pi}{2}\right)^6 + 3 \left(\frac{\mu\pi}{2}\right)^2}{2 \left[1 - \left(\frac{\mu\pi}{2}\right)^4 \right]^2} \right]. \quad (38)$$

Some computations show that the right-hand side of (38) is strictly positive (at least) when $\frac{\mu\pi}{2} < 0.65$, so in particular, when $\mu < 0.4$. This concludes the proof. \square

For the sake of illustration, in Table 3 we give the numerical approximation of G_n , for odd values of $n \in \mathbb{N}$ up to $n = 19$, when $\mu = 1.739 \times 10^{-3}$ (as in (13)):

n	1	3	5	7	9	11	13	15	17	19
G_n	0.9999	-0.1111	0.0399	-0.0204	0.0123	-0.0082	0.0059	-0.0044	0.0034	-0.0027

Table 3: Numerical values of the integral G_n in (29), for some odd values of $n \in \mathbb{N}$.

In fact, for every $\mu \geq 0$ we know that $G_n \rightarrow 0$ as $n \rightarrow \infty$, as a direct consequence of the Riemann-Lebesgue Theorem. This is quite visible also in Table 3.

Our second technical result gives a qualitative property of the graph of $\Gamma_n(\rho)$.

Lemma 5.2. *For all integer $n \geq 1$, the map $\rho \mapsto \Gamma_n(\rho)$ is strictly convex.*

Proof. It suffices to analyze the case when $L = \pi$, and so:

$$\Gamma_n(\rho) = \int_0^{\pi} \sqrt{1 + \left[\frac{q}{H} \left(x - \frac{\pi}{2} \right) + n\rho \cos(nx) \right]^2} dx - L_c \quad \forall \rho \in \mathbb{R}, \quad \forall n \in \mathbb{N}.$$

After differentiating under the integral sign we obtain the following:

$$\Gamma'_n(\rho) = \int_0^\pi \frac{n \cos(nx) \left[\frac{q}{H} \left(x - \frac{\pi}{2} \right) + n\rho \cos(nx) \right]}{\sqrt{1 + \left[\frac{q}{H} \left(x - \frac{\pi}{2} \right) + n\rho \cos(nx) \right]^2}} dx, \quad (39)$$

$$\Gamma''_n(\rho) = \int_0^\pi \frac{[n \cos(nx)]^2}{\left[1 + \left(\frac{q}{H} \left(x - \frac{\pi}{2} \right) + n\rho \cos(nx) \right)^2 \right]^{3/2}} dx,$$

for $\rho \in \mathbb{R}$ and $n \in \mathbb{N}$. Therefore, $\Gamma''_n(\rho) > 0$, for every $n \geq 1$ and $\rho \in \mathbb{R}$, so that Γ_n is a strictly convex function all over \mathbb{R} . \square

In view of (39), we see that

$$\Gamma'_n(0) = \frac{nq}{H} \int_0^\pi \frac{\left(x - \frac{\pi}{2} \right) \cos(nx)}{\sqrt{1 + \left(\frac{q}{H} \right)^2 \left(x - \frac{\pi}{2} \right)^2}} dx. \quad (40)$$

If n is even, then the integrand in (40) is skew-symmetric with respect to $x = \pi/2$ and hence

$$\Gamma'_n(0) = 0 \quad \text{for even } n. \quad (41)$$

If n is odd, then we make the substitution $t = x - \frac{\pi}{2}$ and we note that

$$\cos\left(nt + \frac{n\pi}{2}\right) = \begin{cases} -\sin(nt), & \text{if } n \equiv 1 \pmod{4} \\ \sin(nt), & \text{if } n \equiv 3 \pmod{4}, \end{cases}$$

for all $n \geq 1$ and $t \in \left[-\frac{\pi}{2}, \frac{\pi}{2}\right]$. Therefore, after setting $\mu = \frac{q}{H}$, we see that $\Gamma'_n(0) = -2\mu n \delta(n) G_n$ if n is odd. From (31) and Lemma 5.1 we then infer that

$$\Gamma'_n(0) < 0 \quad \text{for odd } n. \quad (42)$$

Since $\Gamma_n(0) = 0$ for all n , Theorem 2.1 follows by combining Lemma 5.2 with (41) and (42).

Acknowledgments. The first author is partially supported by the PRIN project *Partial differential equations and related analytic-geometric inequalities* and by GNAMPA-INdAM.

References

- [1] I. Ekeland and R. Temam. *Convex Analysis and Variational Principles*. North-Holland, Amsterdam, 1976.
- [2] A. Ferrero and F. Gazzola. A partially hinged rectangular plate as a model for suspension bridges. *Cont. Dynam. Syst. A*, 35:5879–5908, 2015.
- [3] F. Gazzola, M. Jleli, and B. Samet. On the Melan equation for suspension bridges. *Journal of Fixed Point Theory and Applications*, 16(1-2):159–188, 2014.
- [4] F. Gazzola, Y. Wang, and R. Pavani. Variational formulation of the Melan equation. *Mathematical Methods in the Applied Sciences*, 2017. DOI: 10.1002/mma.3962.

- [5] J. Luco and J. Turmo. Effect of hanger flexibility on dynamic response of suspension bridges. *J. Engineering Mechanics*, 136:1444–1459, 2010.
- [6] J. Melan. *Theory of Arches and Suspension Bridges (Myron Clark, London, 1913)*, volume 2. Myron Clark Publ. Comp. London, 1913.
- [7] S. A. Nazarov, A. Stylianou, and G. Sweers. Hinged and supported plates with corners. *Zeitschrift für Angewandte Mathematik und Physik (ZAMP)*, 63(5):929–960, 2012.
- [8] W. Podolny. *Cable-suspended bridges*. In: Structural Steel Designer’s Handbook: AISC, AASHTO, AISI, ASTM, AREMA, and ASCE-07 Design Standards. By R.L. Brockenbrough and F.S. Merritt, 5th Edition, McGraw-Hill, 2011.
- [9] B. Semper. Finite element methods for suspension bridge models. *Computers Math. Applic.*, 26:77–91, 1993.
- [10] B. Semper. A mathematical model for suspension bridge vibration. *Mathematical and Computer Modelling*, 18:17–28, 1993.
- [11] B. Semper. Finite element approximation of a fourth order integro-differential equation. *Appl. Math. Lett.*, 7:59–62, 1994.
- [12] G. Sweers. A survey on boundary conditions for the biharmonic. *Complex Variables and Elliptic Equations*, 54(2):79–93, 2009.
- [13] S. Timoshenko. Theory of suspension bridges - Part I. *Journal of the Franklin Institute*, 235:213–238, 1943.
- [14] S. Timoshenko. Theory of suspension bridges - Part ii. *Journal of the Franklin Institute*, 235:327–349, 1943.
- [15] T. Von Kármán and M. A. Biot. *Mathematical methods in engineering: an introduction to the mathematical treatment of engineering problems*. McGraw-Hill, 1940.
- [16] G. Wollmann. Preliminary analysis of suspension bridges. *J. Bridge Eng.*, 6:227–233, 2001.